




Lab #1 - Single-Point and Differential Positioning

Cheng Huang*

1 Task 1

1.1 Assumptions

1.1.1 *Theoretical Assumptions*

1. There is no correlation between observations.
2. Measurement errors have a symmetrical distribution. 
3. The frame center's coordinate is (0,0,0).
4. Receiver clock must be precise enough, the absolute clock error is no larger than 10ms.
5. The iteration process can converge and the loss of precision caused by Taylor Expansion can be neglected.

1.1.2 *Empirical Assumptions*

1. Observations are equally weighted.
2. The data has already been corrected for tropospheric error, group delay, satellite clock offset and drift.
3. Reference station's coordinate is accurate.

1.2 Data Decoding

Given data files can be classified into two kinds - observation file and satellite file. Both file types are using the same coding format which allocates each element 64-bit(double). Besides, for both file types, each second of data contains 12 channels. So the basic strategy for data

*E-mail: cheng.huang1@ucalgary.ca

decoding is to use "fread" function in MATLAB with the third parameter set to "double". Then, assigning the value of each column to the corresponding variable which is showed in table one and two.

TABLE 1
Observation File Variables

m	Number of epochs
prn	Satellite PRN
t_0	GPS time of observation (seconds)
prange	C/A code pseudorange (m)
cp_l1	L1 carrier phase measurement (L1 cycles)
doppler_l1	Doppler of L1 carrier (Hertz)
cp_l2	L2 carrier phase measurement (L2 cycles)

TABLE 2
Satellite File Variables

prn	Satellite PRN
t_0	GPS time of observation (seconds)
x	X Satellite Coordinate (m)
y	Y Satellite Coordinate (m)
z	Z Satellite Coordinate (m)
xv	X Satellite Velocity (m/s)
yv	Y Satellite Velocity (m/s)
zv	Z Satellite Velocity (m/s)

1.3 Single Point Positioning(SPP)

After decoding the binary file, Parametric Least-squares algorithm is implemented to solve for the coordinates of the remote receiver and determine the position error in ENU frame. The flowchart is showed in Figure 1.

As has showed in the flowchart above, here is a little more explanation of the details. "Data Matching" means connecting pseudorange measurements and satellite positions by matching PRN from these two files. "PLSQ-SPP" means Single Point Positioning by using Parametric Least-

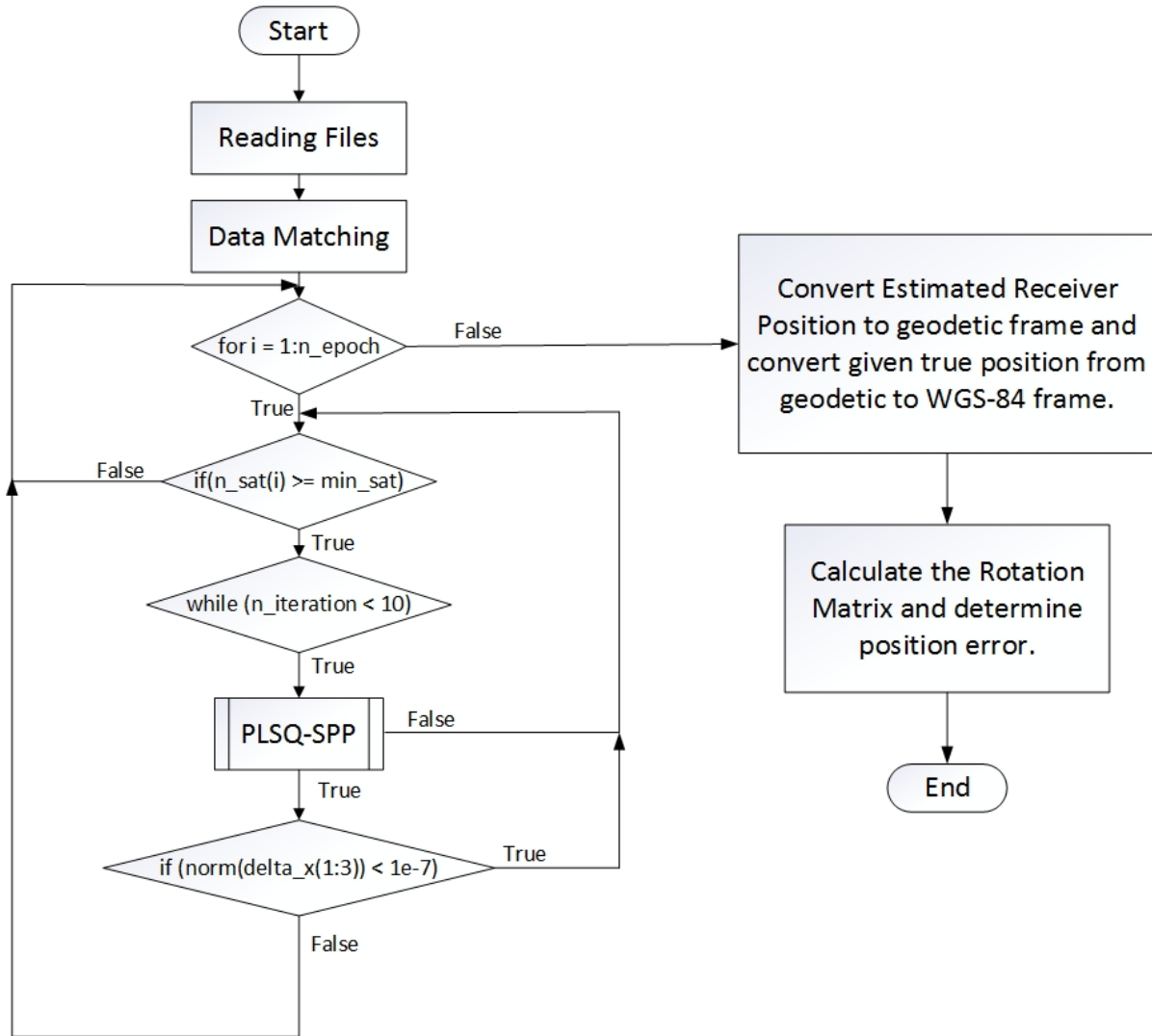


FIGURE 1

Flowchart of SPP and position error determination

squares. Since this is not the main point of this lab, no further illustration is presented in this report. However, it should still be noted that least square estimation is conducted independently on each epoch which means that no prior information is introduced in data processing. Frame transforming are involved with two parts. The first part is converting the estimated receiver positions from WGS-84 to geodetic frame in order to compute the rotation matrix for ENU frame. The rotation matrix formula is as follows.

$$R = \begin{pmatrix} -\sin(\lambda) & \cos(\lambda) & 0 \\ -\sin(\phi) * \cos(\lambda) & -\sin(\phi) \sin(\lambda) & \cos(\phi) \\ \cos(\phi) \cos(\lambda) & \cos(\phi) \sin(\lambda) & \sin(\phi) \end{pmatrix} \quad (1.1)$$

The second part is to convert the given true position from geodetic frame to WGS-84 frame. The ellipsoid semi-major axis and ellipsoid flattening for WGS-84 frame are 6378137(m) and 1/298.257223563 respectively.

After all the conversion, the position error(true accuracy) can be written as:

$$\sigma_{TRUE} = R * (x_{ref} - XR) \quad (1.2)$$

Where R is the rotation matrix, x_ref is the given true position in WGS-84 frame, XR is the estimated receiver position in WGS-84 frame. In the same time, the estimated standard deviations(positive and negative) are also calculated to form an "envelope" to compare with the true accuracy. In the process of PLSQ, the posteriori variance of unit weight is determined as:

$$\hat{\sigma}_0 = \frac{r^T * C_z^{-1} * r}{n - m} \quad (1.3)$$

where the variance-covariance matrix of measurement C_z is assumed to be identity matrix.

The posteriori variance-covariance matrix of states are determined as:

$$C_{\hat{x}} = \hat{\sigma}_0 (H^T * C_z^{-1} * H)^{-1} \quad (1.4)$$

The "envelope" can be defined as:

$$\begin{aligned} -\sqrt{C_{\hat{x}}(1,1)} &\leq \hat{\sigma}_x \leq \sqrt{C_{\hat{x}}(1,1)} \\ -\sqrt{C_{\hat{x}}(2,2)} &\leq \hat{\sigma}_y \leq \sqrt{C_{\hat{x}}(2,2)} \\ -\sqrt{C_{\hat{x}}(3,3)} &\leq \hat{\sigma}_z \leq \sqrt{C_{\hat{x}}(3,3)} \end{aligned} \quad (1.5)$$



1.4 Results and Analysis

By computing the true and estimated error components, time series of these errors are plotted in East, North, Up direction separately.

As is showed in Figure 2, it's easy to find out that estimated accuracy accords with true accuracy better in East and North direction than in Up direction. This result reflects the fact that GNSS position error is relatively large in vertical direction because of the correlation between height measurement and receiver clock offset. It should also be noticed that "true accuracy" here has a bias from 0 which indicates that there are some non-Gaussian distributed errors.

As for the difference between the true and estimated accuracy, "true accuracy" here means the gap between estimated receiver position and the true position which should be described as error strictly, "estimated accuracy" means posteriori standard deviation of position accuracy. It should be noted that the absolute value of true accuracy refers to RMSE of the estimated receiver position.

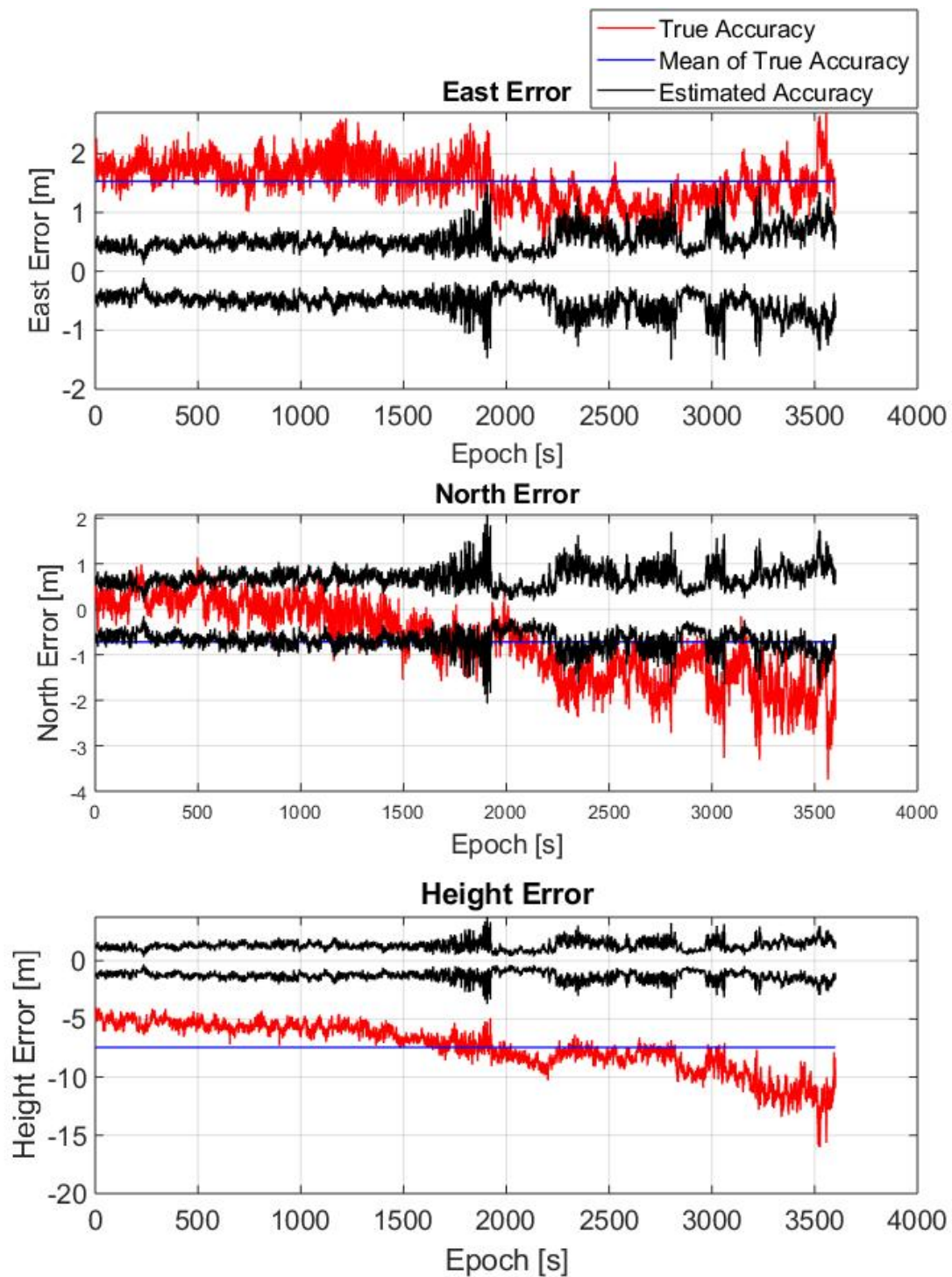



FIGURE 2

True accuracy vs. estimated accuracy

The discrepancies between the true and estimated accuracy can be influenced by all theoretical assumptions. Those are the prerequisites to implement LS algorithm on pseudorange positioning. Here are some justifications on some assumptions:

- Assumption 1: if the measurements are correlated to each other, error propagation law is not applicable any more. \hat{C}_x will be formed in another way, so the difference between the true accuracy and estimated accuracy changes. 
- Assumption 4: generally speaking, 1ms absolute receiver clock error can cause 1m pseudorange error. If absolute receiver clock error is larger than 10ms, then pseudorange error would be larger than 10m which would result in traditional four states LS algorithm invalid. Thus, \hat{C}_x and XR will be both incorrect.

2 Task 2

2.1 Assumptions

2.1.1 Theoretical Assumptions

1. The frame center's coordinate is (0,0,0).

2.1.2 Empirical Assumptions

1. Observations are equally weighted.

2.2 DOP Computation

DOP Computation is conducted in every epoch data processing. In each LS estimation, the cofactor matrix is formed to strictly measure the satellite geometry:

$$Q_x = (H^T * H)^{-1} \quad (2.1)$$

Based on covariance propagation law, the cofactor matrix is transformed to topocentric local coordinate system as follows.

$$Q_{x_enu} = R * Q_x * R^T \quad (2.2)$$

According to (1.7), EDOP(East direction DOP), NDOP(North direction DOP), VDOP(Vertical DOP), HDOP(Horizontal DOP) and PDOP(3D position DOP) are computed as follows:

$$\begin{aligned} EDOP &= \sqrt{Q_{x_enu}(1,1)} \\ NDOP &= \sqrt{Q_{x_enu}(2,2)} \\ VDOP &= \sqrt{Q_{x_enu}(3,3)} \\ HDOP &= \sqrt{Q_{x_enu}(1,1) + Q_{x_enu}(2,2)} \\ PDOP &= \sqrt{Q_{x_enu}(1,1) + Q_{x_enu}(2,2) + Q_{x_enu}(3,3)} \end{aligned} \quad (2.3)$$

2.3 Results and Analysis

DOP values and number of visible satellites are plotted as a time series showed in Figure 3.

According to the result of Figure 3, it can be concluded that GPS constellation geometry is better in horizontal than in vertical. And in horizontal specifically, it is better in east direction than in north direction. Compared with accuracy plots in Figure 2, the trends of estimated accuracy is consistent with DOP values. Between epoch 1500 and 2000, there is a peak in DOP plots, accordingly, this is also reflected in estimated accuracy plot. In addition, the mean value of

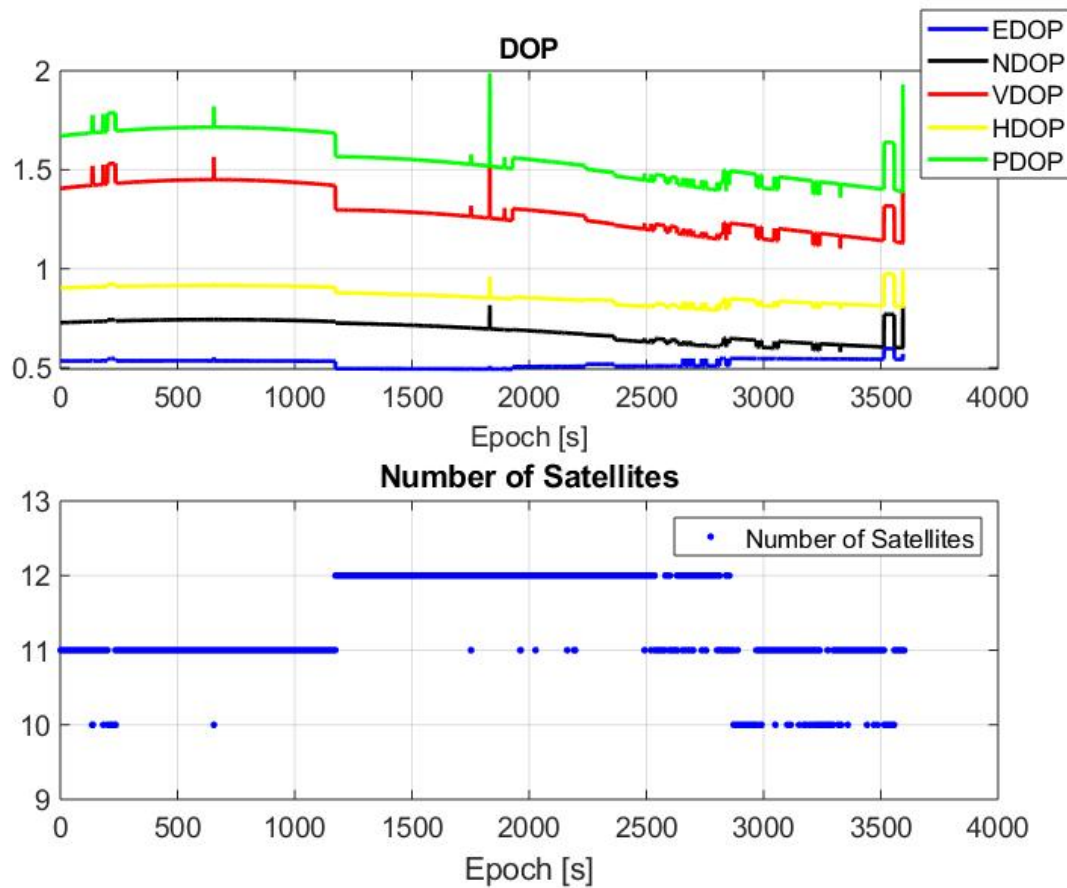


FIGURE 3

DOPs and Number of Visible Satellites

estimated accuracy in east, north and up are 0.53, 0.69 and 1.31 respectively which also accords with the relations between EDOP, NDOP and VDOP. However, the true accuracy is consisted of noise and bias, so the trend is not reflected here.

3 Task 3

3.1 Assumptions

3.1.1 Theoretical Assumptions

1. There is no correlation between observations.
2. Measurement errors have a symmetrical distribution.
3. The frame center's coordinate is (0,0,0).
4. Receiver clock must be precise enough, the absolute clock error is no larger than 10ms.
5. The iteration process can converge and the loss of precision caused by Taylor Expansion can be neglected.

3.1.2 Empirical Assumptions

1. Observations are equally weighted.
2. The data has already been corrected for tropospheric error, group delay, satellite clock offset and drift.

3.2 Satellite Residual and Elevation Angle Computation

In LS solution, once the final state estimate is obtained, the estimated measurement residuals can be computed as:

$$\hat{r} = z - f(x_0) - H * \hat{x} \quad (3.1)$$

where z is pseudorange measurement. $f(x_0)$ is the known vector which refers to geometric distance and ionosphere delay between satellite and receiver in this case.

Elevation angle is computed in the topocentric local coordinates. First, converting satellite coordinate X_S to topocentric local coordinates by:

$$X_{s_enu} = R * (X_S - X_R) \quad (3.2)$$

Elevation angle is computed as:

$$ele = \arctan\left(\frac{X_{s_enu}(3)}{\sqrt{X_{s_enu}(1)^2 + X_{s_enu}(2)^2}}\right) \quad (3.3)$$

3.3 Results and Analysis

Satellite observation residuals are plotted as a time series in Figure 4. Meanwhile, satellite residuals are also plotted as a function of satellite elevation angle in Figure 5.

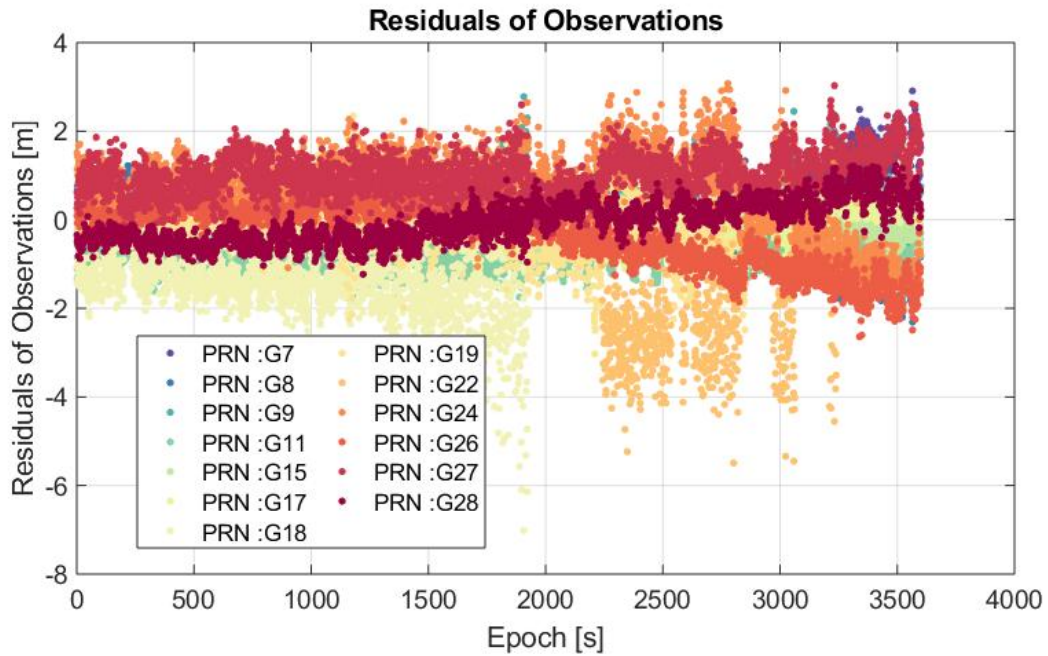


FIGURE 4

Satellite Residuals as Time Series

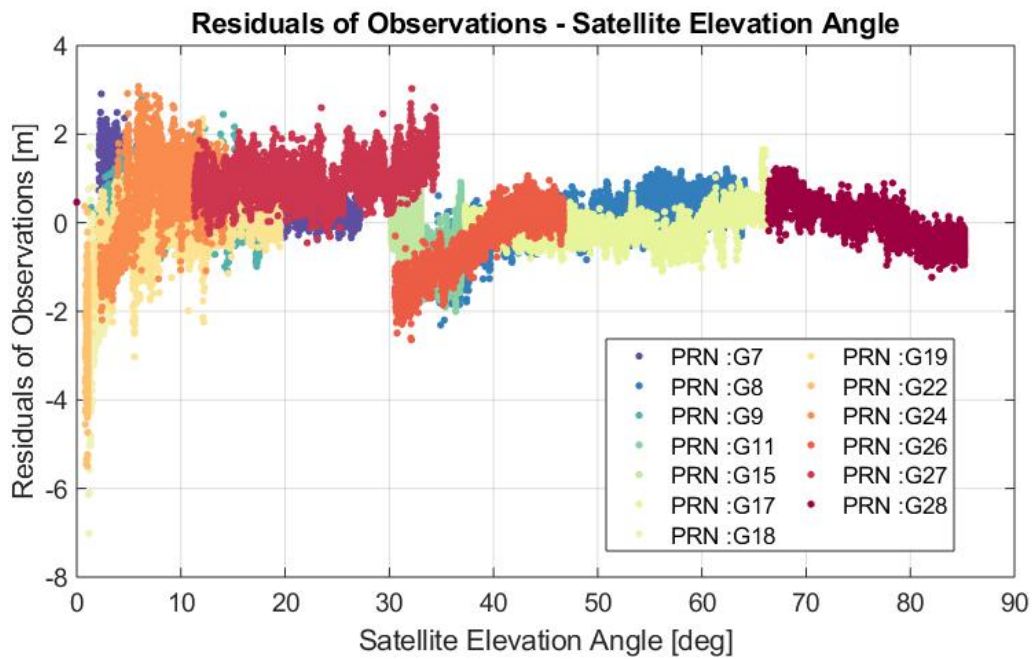


FIGURE 5

Satellite Residuals as a Function of Satellite Elevation Angle

Comparing Figure 4 and Figure 5, it can be seen that satellites with low elevation angle like G18 and G22 have larger residuals compared with other satellites with high elevation angles. From the comparison, multipath effect and ionospheric errors are showed in the trends. Generally speaking, satellites with low elevation angles are more likely to be influence by multipath effect and ionospheric errors.

4 Task 4

4.1 Satellite Picking

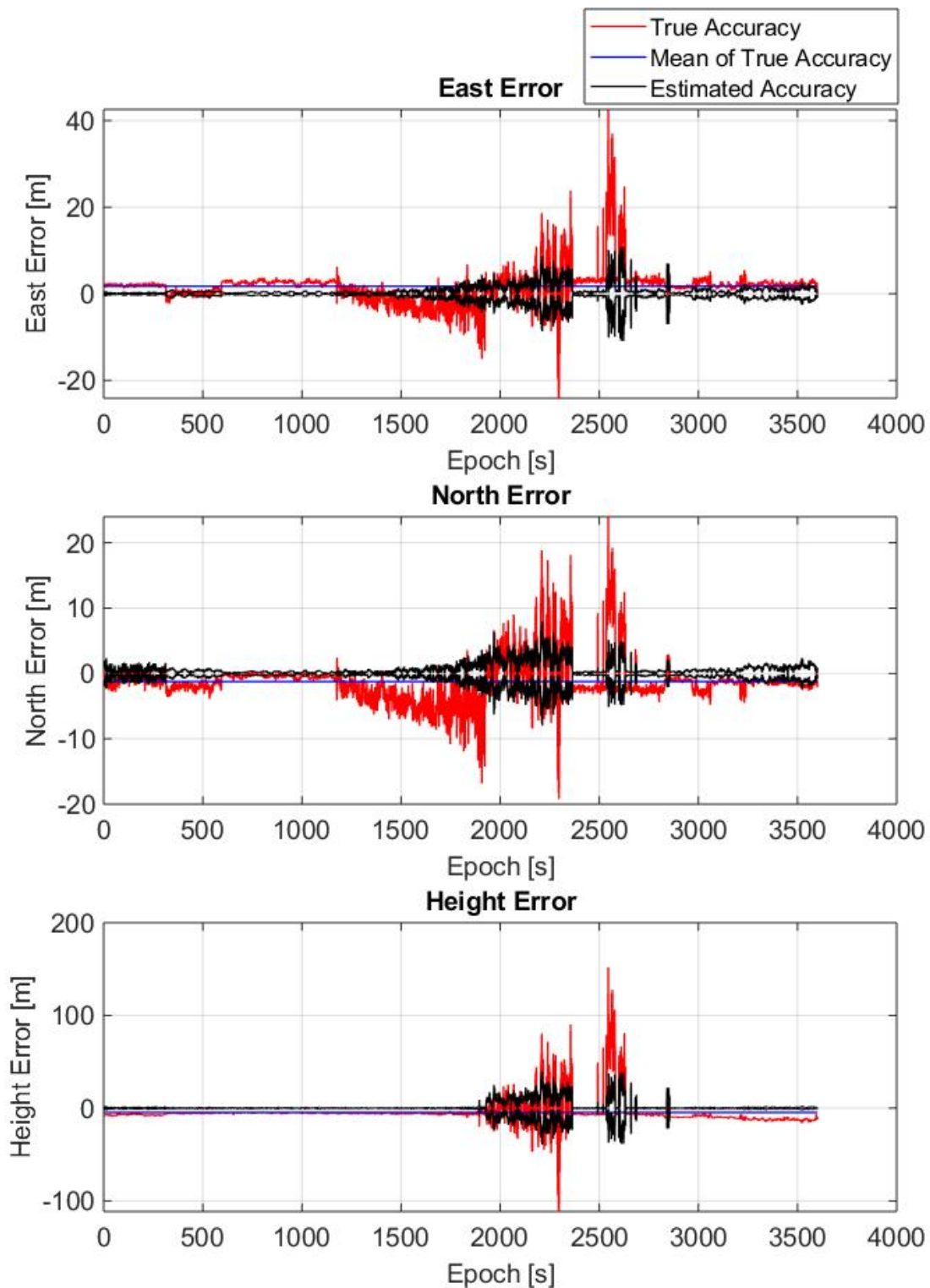
Given that task 4 is a derivation of the former tasks, so the assumptions are the same as task 3. The methodology used here is finding all the possible combinations of the visible satellites in each epoch and picking out the combination that returns the highest PDOP value.

To fully understand the impact of satellite geometry on the accuracy, a control experiment which picks out the combination that returns the smallest DOP value is set.

4.2 Results and Analysis

The results are showed in Figure 6-13. Comparing Figure 6&7 with Figure 2, Figure 8&9 with Figure 3, conclusion can be drawn that no matter which satellite picking scheme we use, five satellites' geometry will not be better than all visible satellites' geometry. It's also reflected on the accuracy plots. Meanwhile, the smaller DOP values are, the better satellite geometry is, the better solution accuracy will be.

However, comparing Figure 10&11 with Figure 4, Figure 12&13 with Figure 5, we can find out that residuals derived from five satellites are smaller than the original method. In some certain epochs, satellites with low elevation angle and large residuals are excluded.

**FIGURE 6**

Accuracy plot with highest DOP values

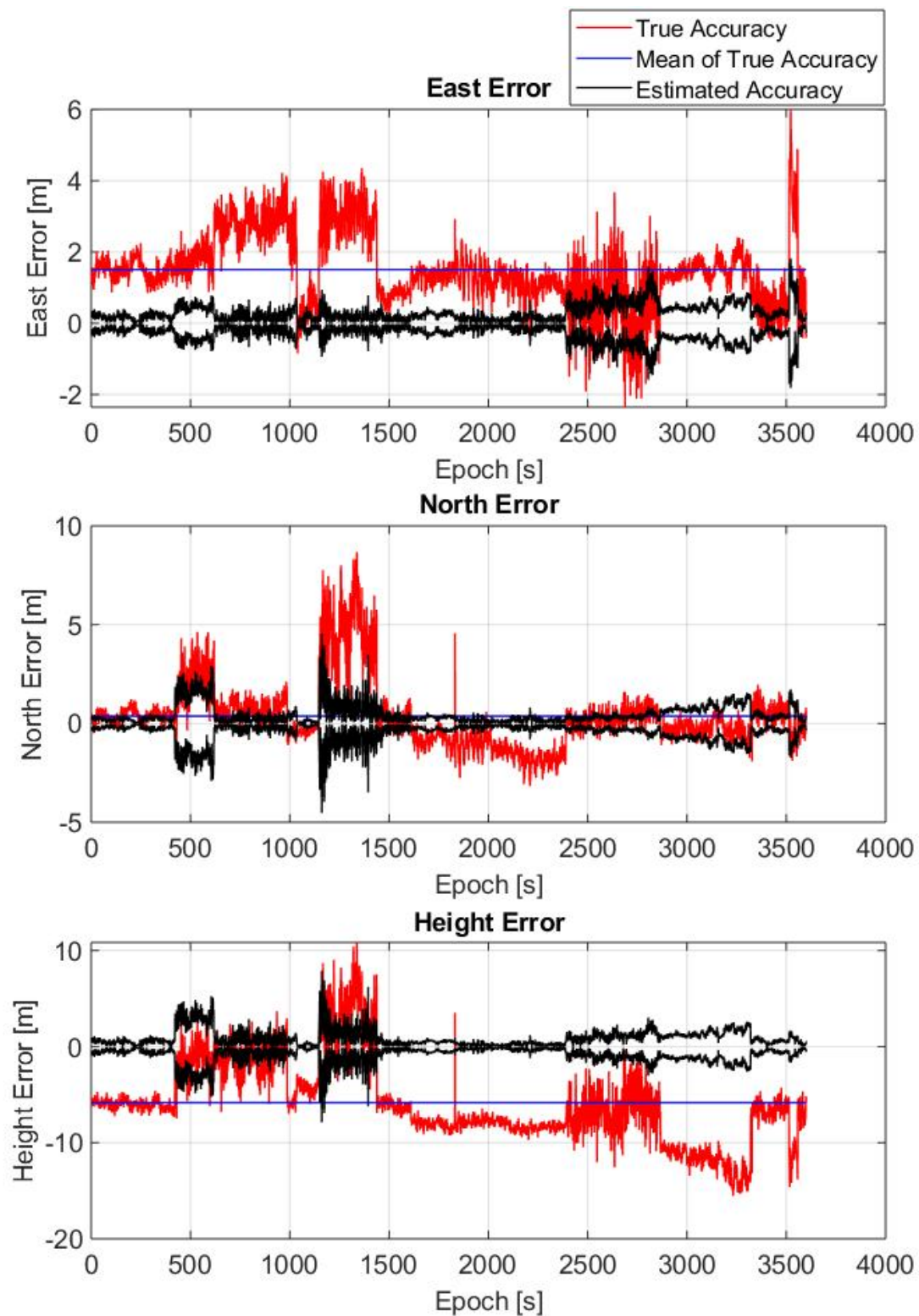


FIGURE 7

Accuracy plot with smallest DOP values

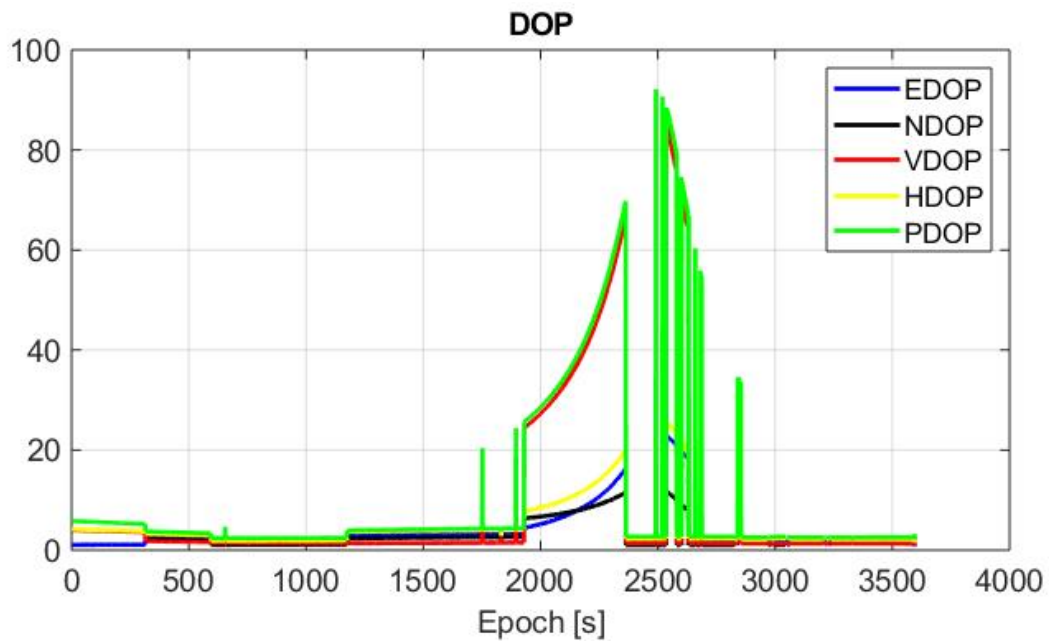


FIGURE 8

DOP plot with highest DOP values

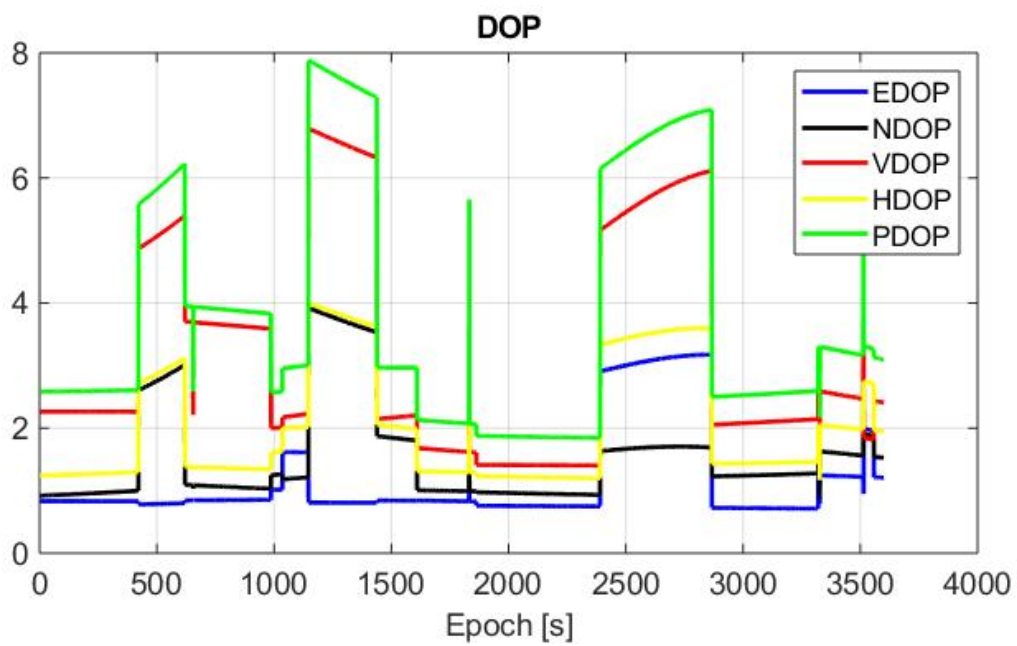
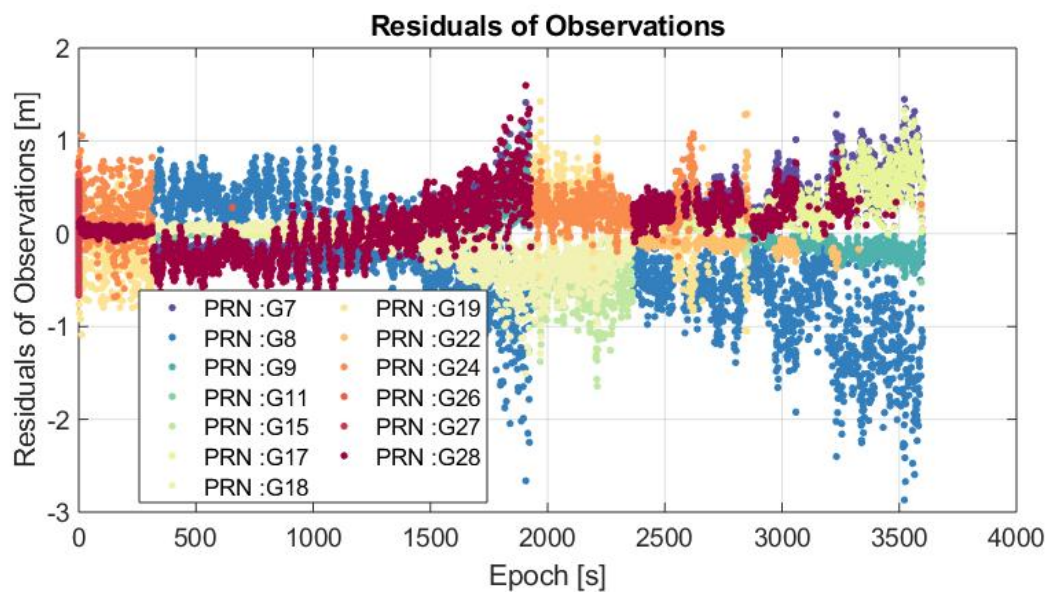
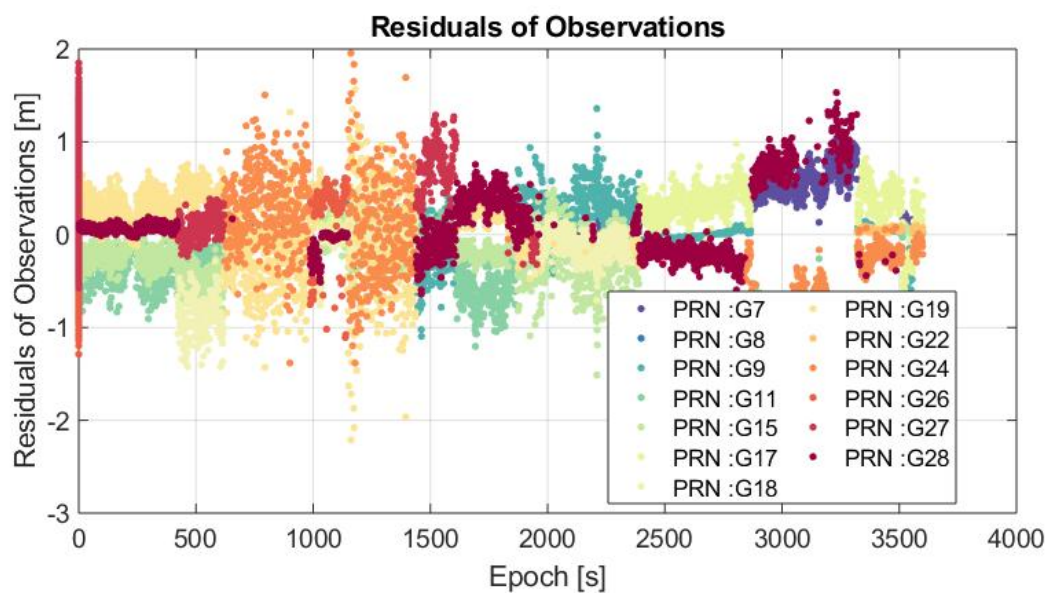


FIGURE 9

DOP plot with smallest DOP values

**FIGURE 10**

Residual plot with highest DOP values

**FIGURE 11**

Residual plot with smallest DOP values

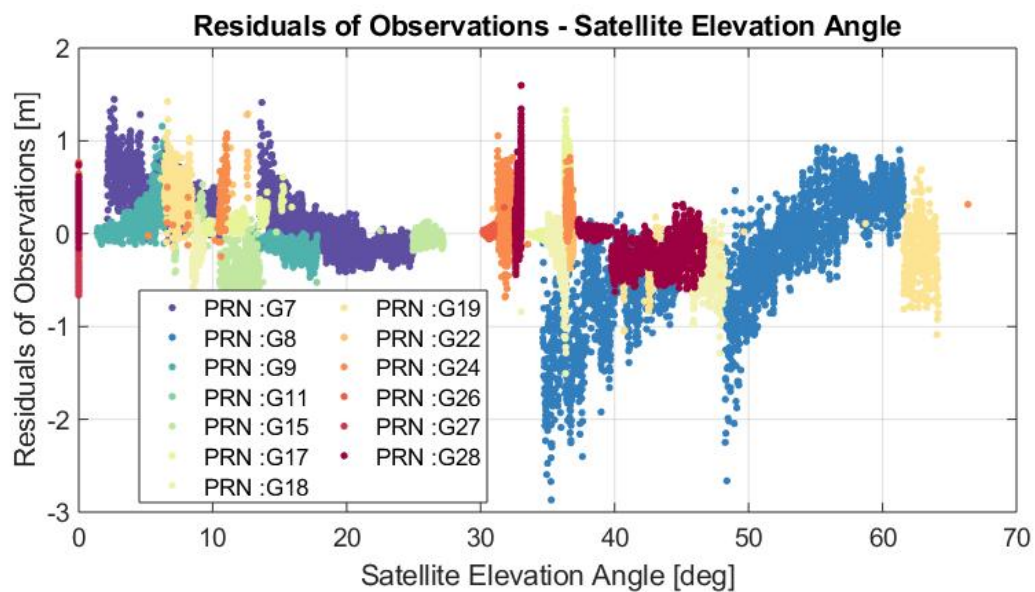


FIGURE 12

Residual-Elevation plot with highest DOP values

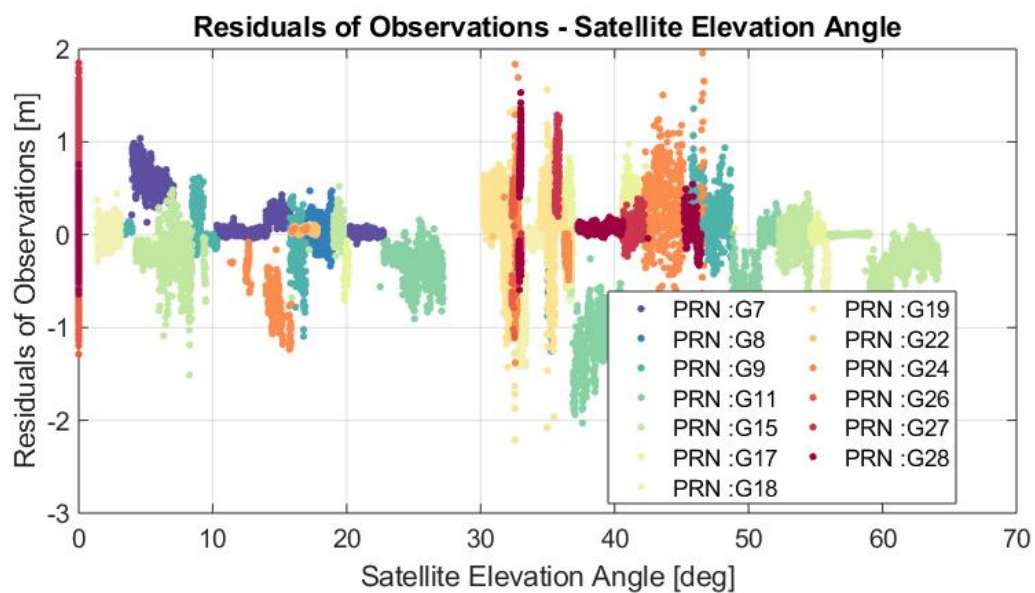


FIGURE 13

Residual-Elevation plot with smallest DOP values

5 Task 5

5.1 Single-differencing vs SPP

Single-differencing here indicates "Between-Receiver Single-differencing" which means that subtracting the pseudorange at reference station from that at remote. In algorithmic implementation details, the design matrix H is the same as SPP; the known term $f(x_0)$ is the difference between the geometric distances between satellite and the two receivers; the observation vector z is the difference between the pseudoranges between satellite and the two receivers. Before the iteration starts, the remote receiver and reference receiver observation files have to be synchronized.

It should be noted that when computing single-differencing residuals, estimated receiver clock offset is also added to the computed residual term.

By doing single-differencing, orbital errors, atmospheric errors and satellite clock errors are reduced.

5.2 Results and Analysis

The single-differencing solution results are showed in Figure 14-17. Compare Figure 14 with Figure 2, we can find out that the mean of accuracy is reduced significantly and the true accuracy is included in the upper and lower range very well which is not the case in Figure 2. This result reflects the fact that single-differencing reduces the orbital errors and atmospheric errors (ionosphere error still remains) which is the main error sources in the given files.

Because the design matrix is the same as SPP, the DOP plot is also the same.

By comparing the Residual plot and the Residual-Elevation plot, we can find out that some large residuals are removed by doing single-differencing. Also, in the Residual-Elevation plot, we can find out that the whole plot is more smooth and consistent compared with Figure 5. (The "Ridge" in Figure 5 is removed by doing single-differencing.) In addition, by comparing the residual plots, it can be drawn that single-differencing wouldn't eliminate the multipath errors.

By picking out the five satellites that gives the highest DOP value, the results are showed in Figure 18-21. By comparing Figure 18-21 with Figure 14-17, we can also come to the conclusion that the smaller DOP values are, the better satellite geometry is, the better solution accuracy will be.

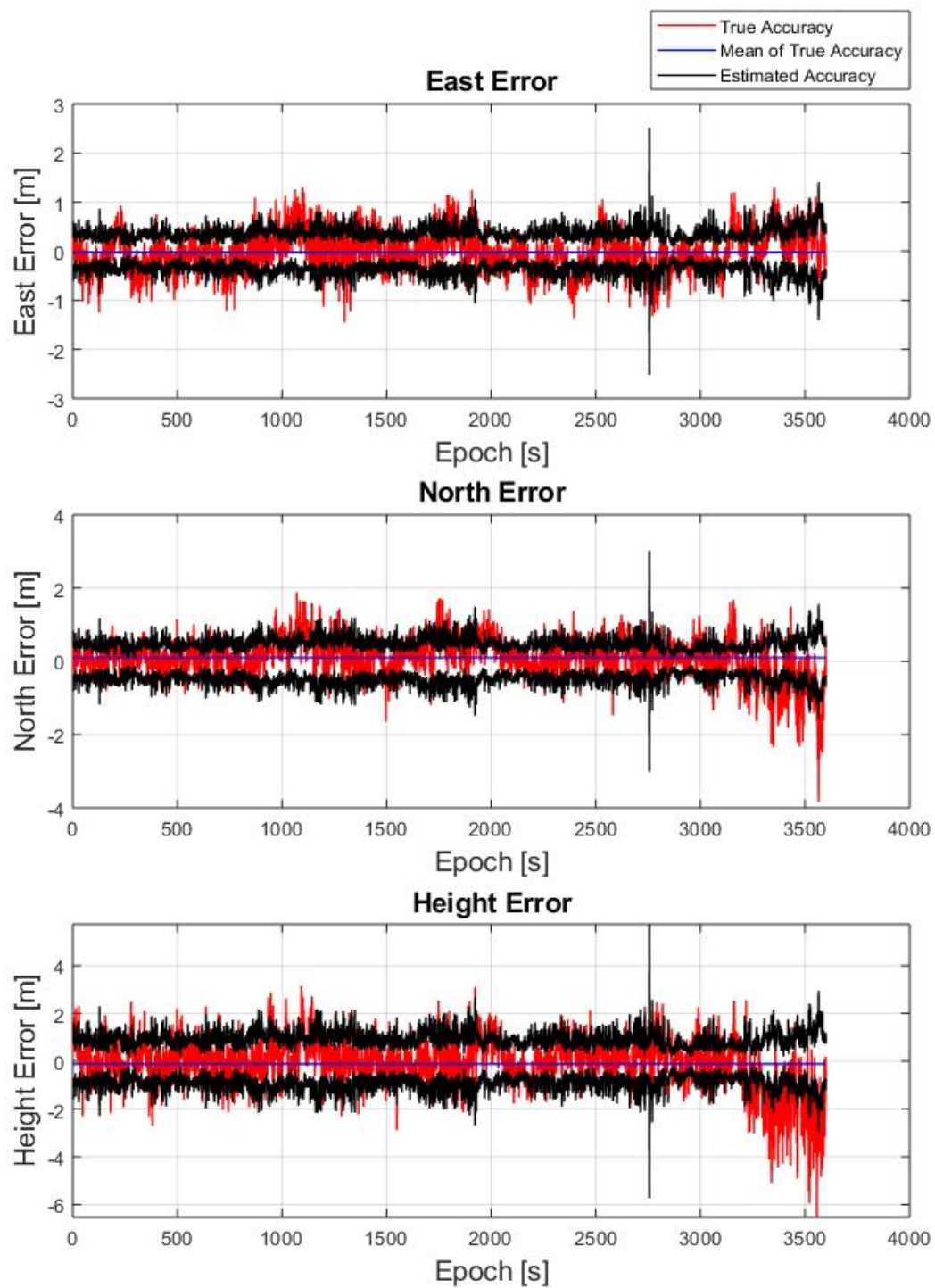


FIGURE 14

Single-differencing accuracy plot

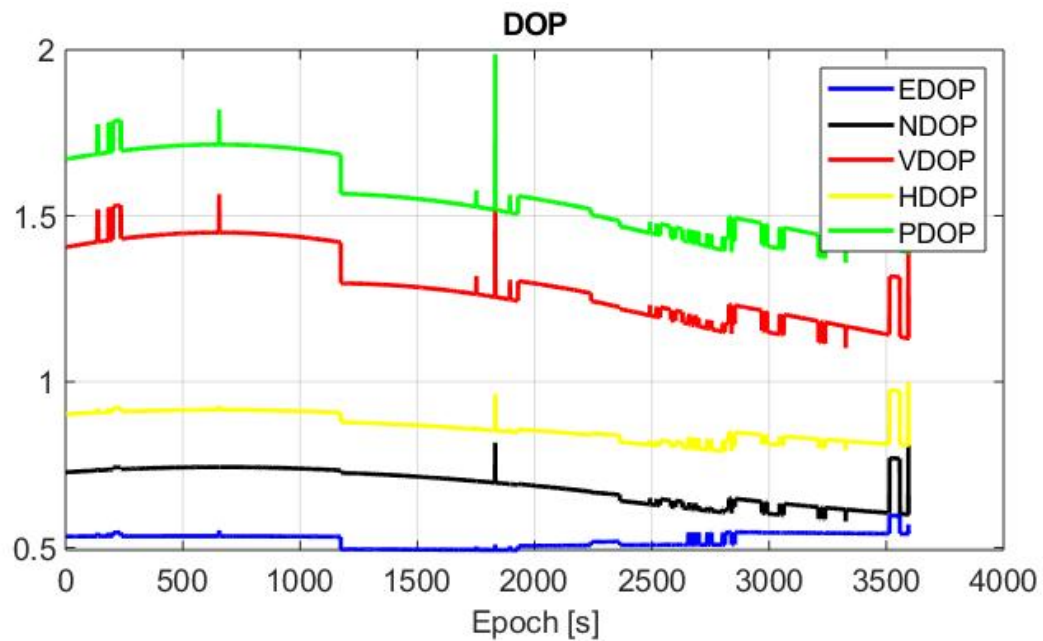


FIGURE 15

Single-differencing DOP plot

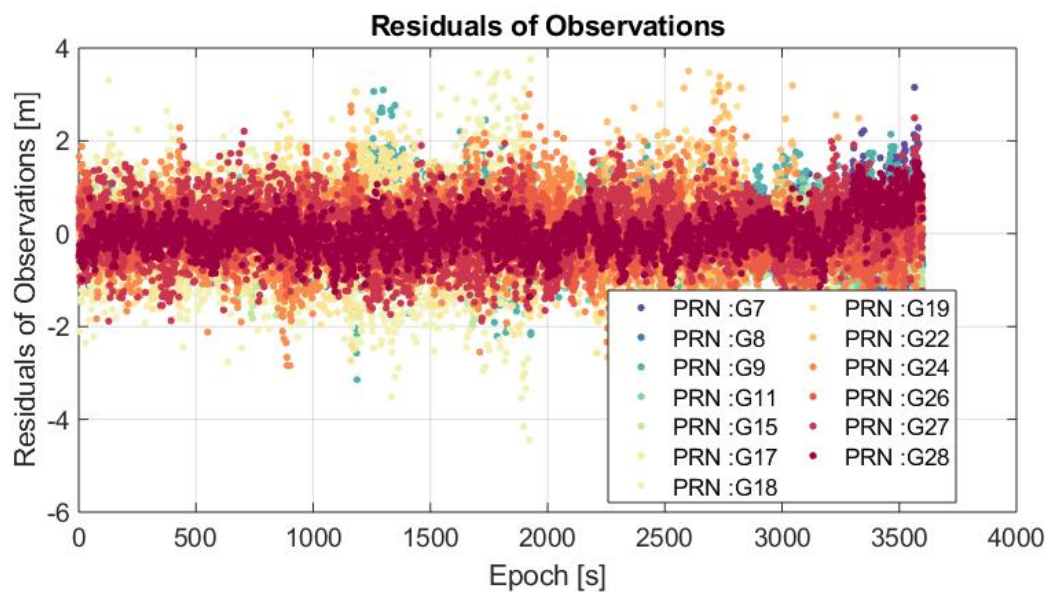
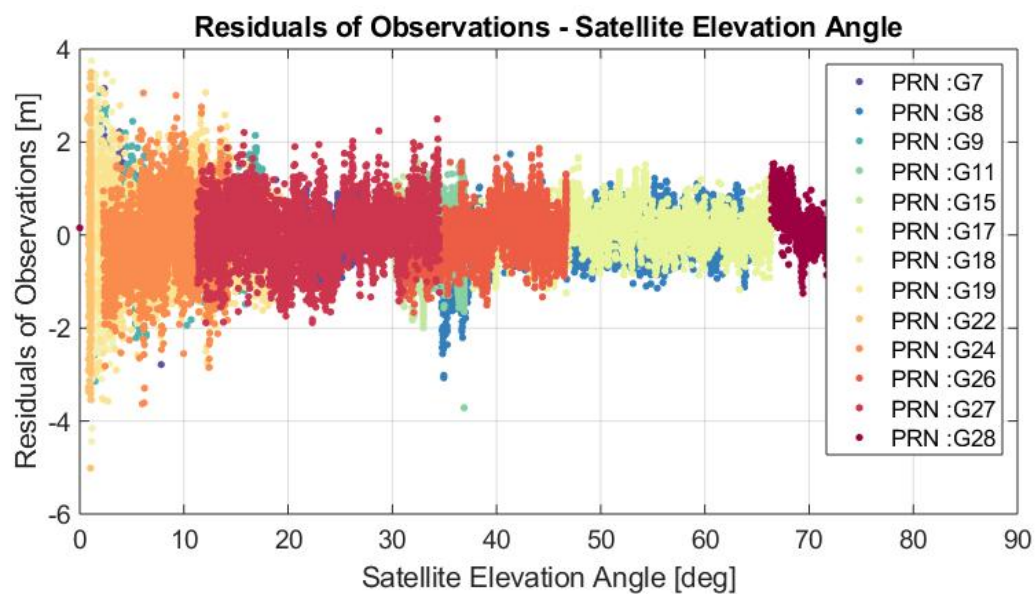


FIGURE 16

Single-differencing residual plot

**FIGURE 17**

Single-differencing Residual-Elevation plot

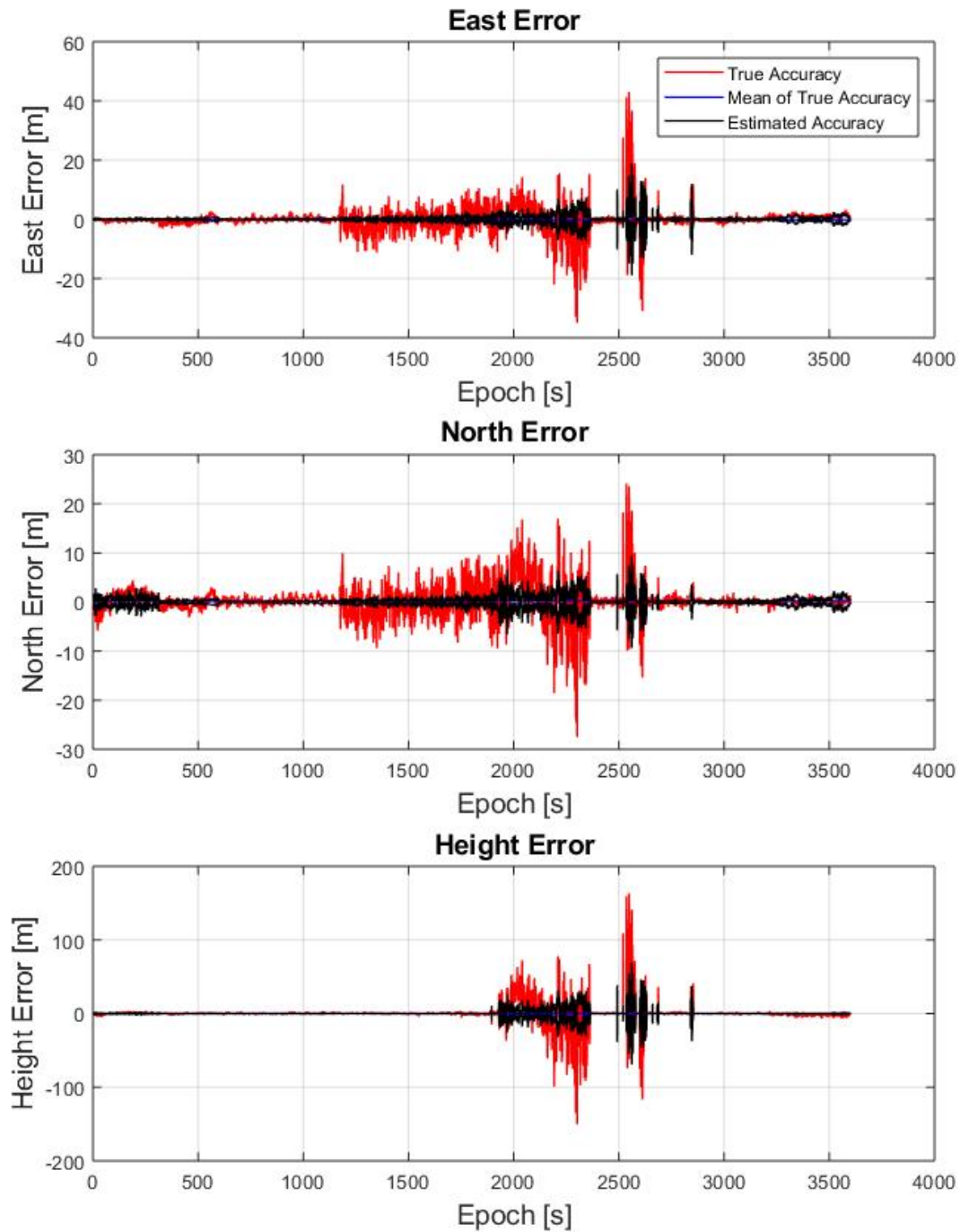


FIGURE 18

Single-differencing accuracy plot with highest DOP values

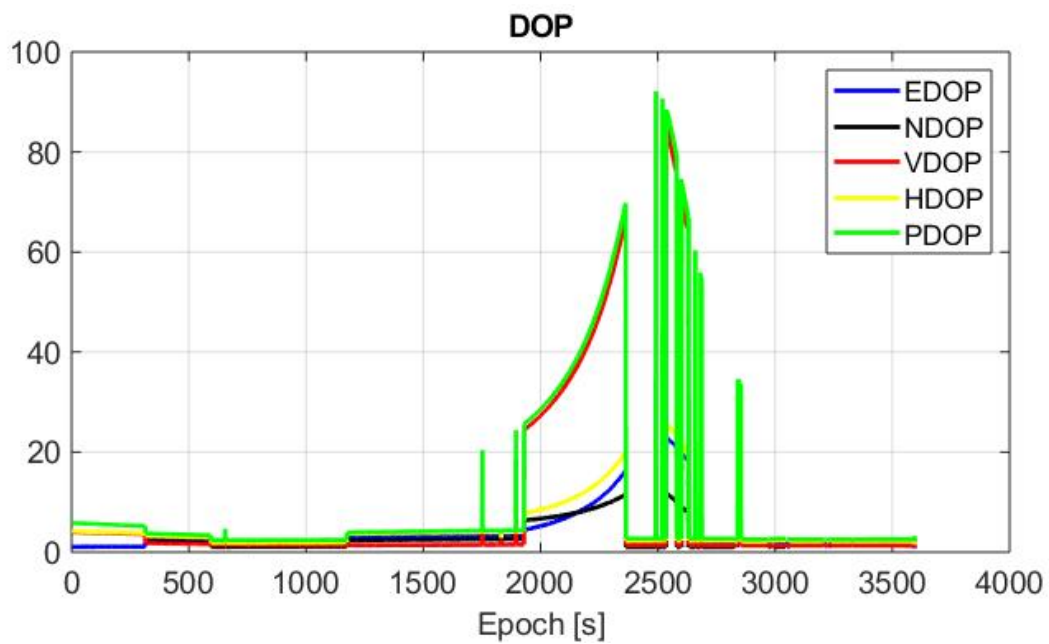


FIGURE 19

Single-differencing DOP plot with highest DOP values

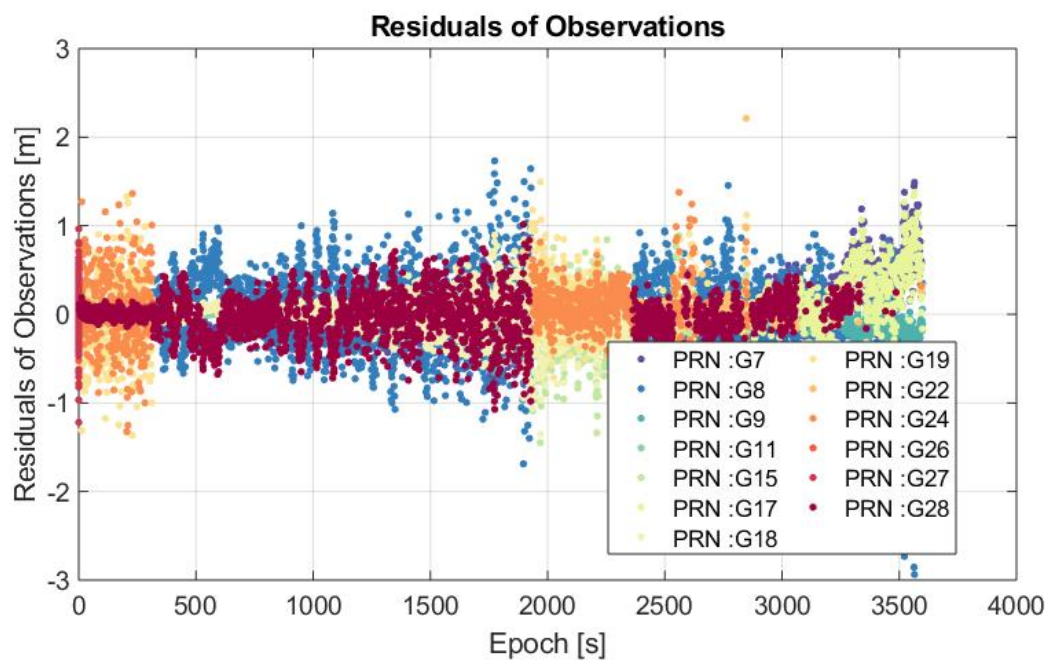
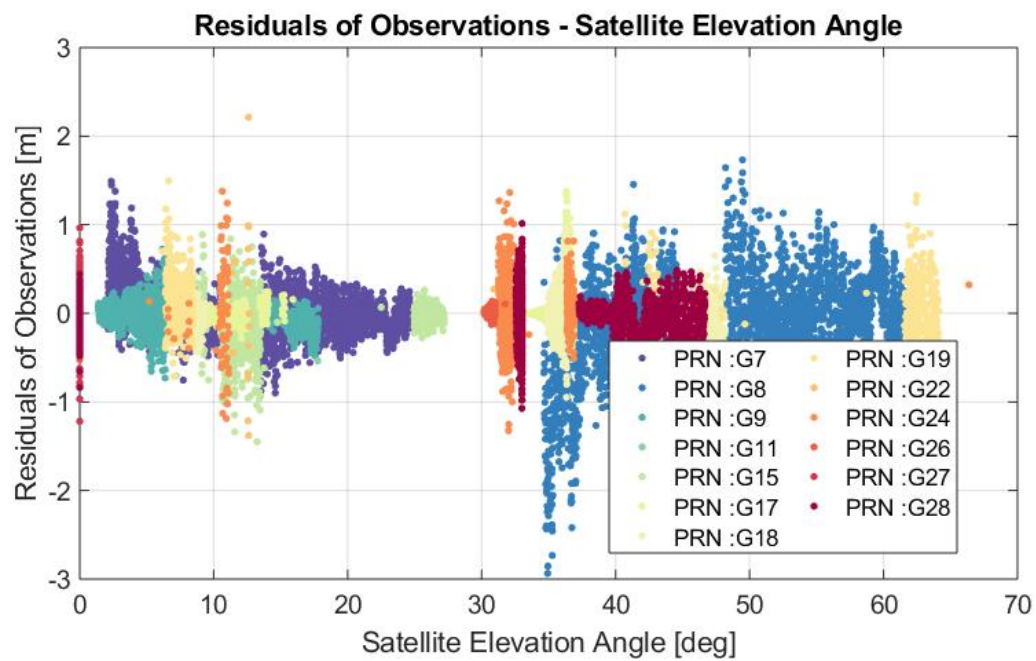


FIGURE 20

Single-differencing residual plot with highest DOP values

**FIGURE 21**

Single-differencing Residual-Elevation plot with highest DOP values

6 Task 6

6.1 Double-differencing vs SPP

Double-differencing here indicates "Between Satellite-Receiver Double-differencing". Double-differencing is the difference between two simultaneous single-differencing observations. There are two ways to implement double-differencing algorithm. For the first way, satellite with the highest elevation angle is chosen as the pivot satellite in each epoch, this method is implemented in "DD_LS_adjustment.m". However, the DOP values will be hard to compute in this method. Then, a more straightforward and easier way is proposed in the second method which constructs a differencing matrix to do all the computation. This method is implemented in "DD_LS_adjustment_B".

In algorithmic implementation details, the design matrix H is:

$$H = \begin{pmatrix} \frac{x_{rem} - x_s^1}{\rho_{rem-s}^1} - \frac{x_{rem} - x_{s_pivot}}{\rho_{rem-s_pivot}} & \frac{y_{rem} - y_s^1}{\rho_{rem-s}^1} - \frac{y_{rem} - y_{s_pivot}}{\rho_{rem-s_pivot}} & \frac{z_{rem} - z_s^1}{\rho_{rem-s}^1} - \frac{z_{rem} - z_{s_pivot}}{\rho_{rem-s_pivot}} \\ \frac{x_{rem} - x_s^2}{\rho_{rem-s}^2} - \frac{x_{rem} - x_{s_pivot}}{\rho_{rem-s_pivot}} & \frac{y_{rem} - y_s^2}{\rho_{rem-s}^2} - \frac{y_{rem} - y_{s_pivot}}{\rho_{rem-s_pivot}} & \frac{z_{rem} - z_s^2}{\rho_{rem-s}^2} - \frac{z_{rem} - z_{s_pivot}}{\rho_{rem-s_pivot}} \\ \frac{x_{rem} - x_s^3}{\rho_{rem-s}^3} - \frac{x_{rem} - x_{s_pivot}}{\rho_{rem-s_pivot}} & \frac{y_{rem} - y_s^3}{\rho_{rem-s}^3} - \frac{y_{rem} - y_{s_pivot}}{\rho_{rem-s_pivot}} & \frac{z_{rem} - z_s^3}{\rho_{rem-s}^3} - \frac{z_{rem} - z_{s_pivot}}{\rho_{rem-s_pivot}} \\ \vdots & \vdots & \vdots \\ \frac{x_{rem} - x_s^n}{\rho_{rem-s}^n} - \frac{x_{rem} - x_{s_pivot}}{\rho_{rem-s_pivot}} & \frac{y_{rem} - y_s^n}{\rho_{rem-s}^n} - \frac{y_{rem} - y_{s_pivot}}{\rho_{rem-s_pivot}} & \frac{z_{rem} - z_s^n}{\rho_{rem-s}^n} - \frac{z_{rem} - z_{s_pivot}}{\rho_{rem-s_pivot}} \end{pmatrix} \quad (6.1)$$

The known term $f(x_0)$ is the difference between the two single-differencing known terms; the observation vector z is the difference between the two single-differencing observation vectors; Before the iteration starts, the remote receiver and reference receiver observation files have to be synchronized.

The differencing matrix is written as:

$$B_{(n-1) \times 2n} = \begin{pmatrix} 1 & -1 & \cdots & 0 & -1 & 1 & \cdots & 0 \\ 1 & 0 & \ddots & 0 & -1 & 0 & \ddots & 0 \\ 1 & 0 & \cdots & -1 & -1 & 0 & \cdots & 1 \end{pmatrix} \quad (6.2)$$

By constructing this B matrix, the pivot satellite will always be the first element in the first observation vector. Thus, the cofactor matrix can be written as:

$$Q_x = (H^T * (B * R * B^T)^{-1} * H)^{-1}$$

By doing double-differencing, the orbital and atmospheric errors are reduced, in the same time, both satellite clock error and receiver clock error are eliminated.

6.2 Results and Analysis

The double-differencing solution results are showed in Figure 22-25. By comparing Figure 22 with Figure 14, we can find out that there is not a big difference. Namely, the major errors have already been eliminated during single-differencing process, or we can say the receiver clock offset is relatively small. However, this is an intuitive conclusion, numerical analysis will be presented in Task 7.

By comparing Figure 23 with Figure 3, it's shown that the DOP values increase by doing double-differencing. This is because double-differencing will result in a loss of degrees of freedom, thus making satellite geometry not as good as the original one.

By comparing Figure 24 and Figure 16, Figure 25 and Figure 17, we can find out that they are almost identical. Because carrier phase solution is not involved in double-differencing here, the superiority of double-differencing is not manifested.

By picking out the five satellites that gives the highest DOP value, the results are showed in Figure 26-29. By comparing Figure 26-29 with Figure 22-25, we can also come to the conclusion that the smaller DOP values are, the better satellite geometry is, the better solution accuracy will be.

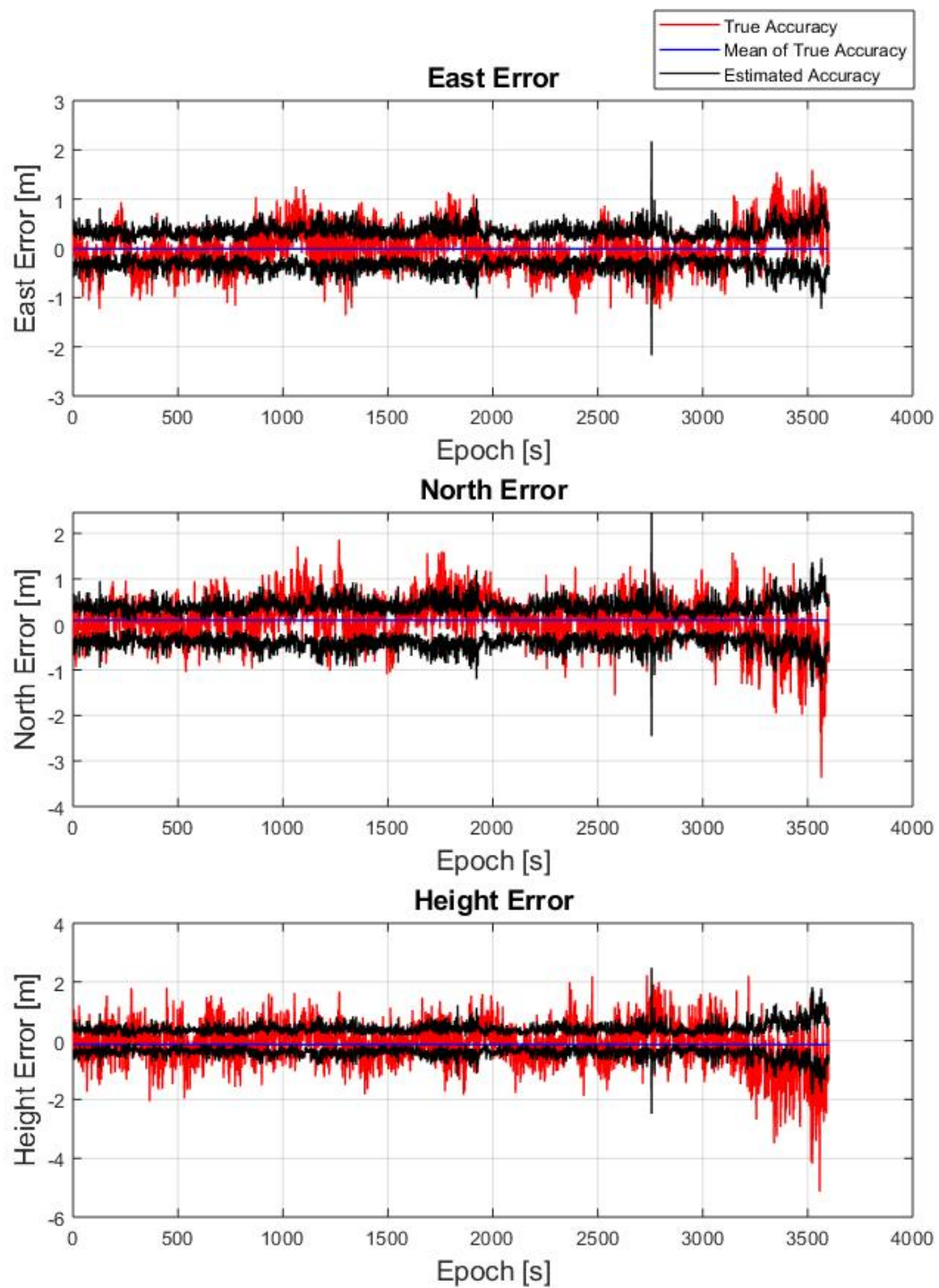


FIGURE 22

Double-differencing accuracy plot

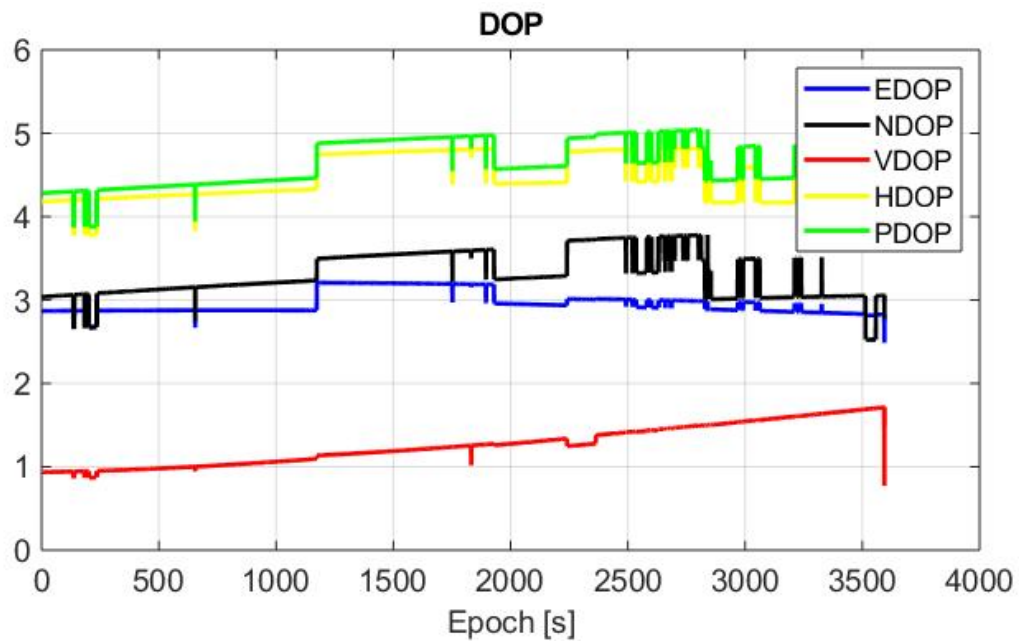


FIGURE 23

Double-differencing DOP plot

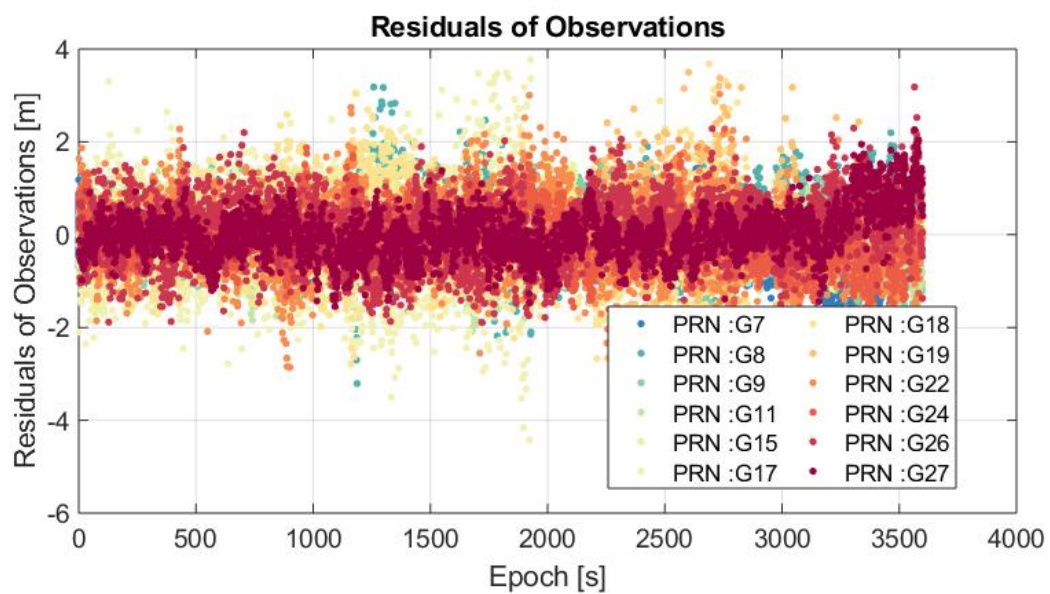


FIGURE 24

Double-differencing residual plot

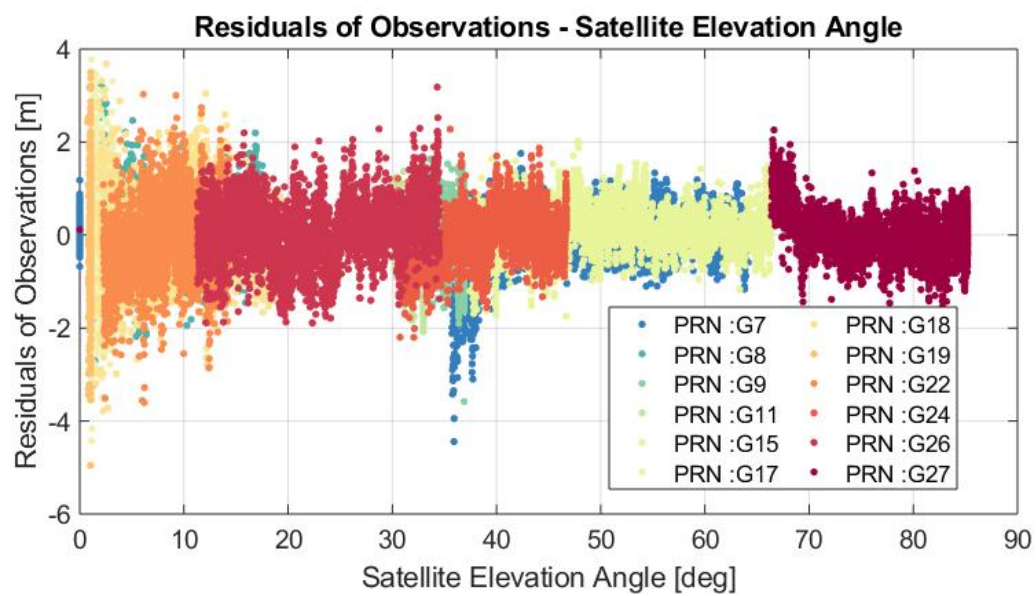


FIGURE 25

Double-differencing Residual-Elevation plot

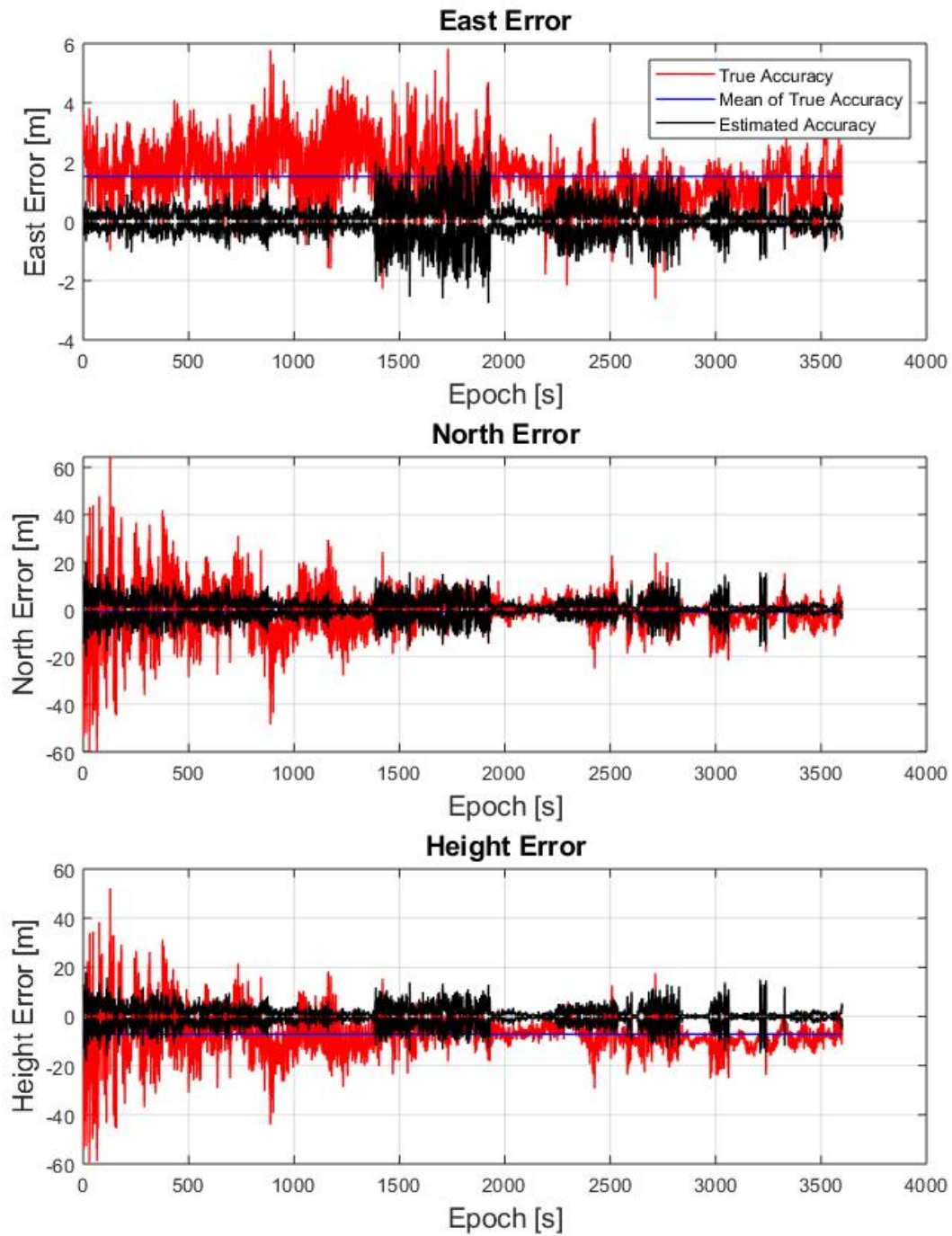


FIGURE 26

Double-differencing accuracy plot with highest DOP values

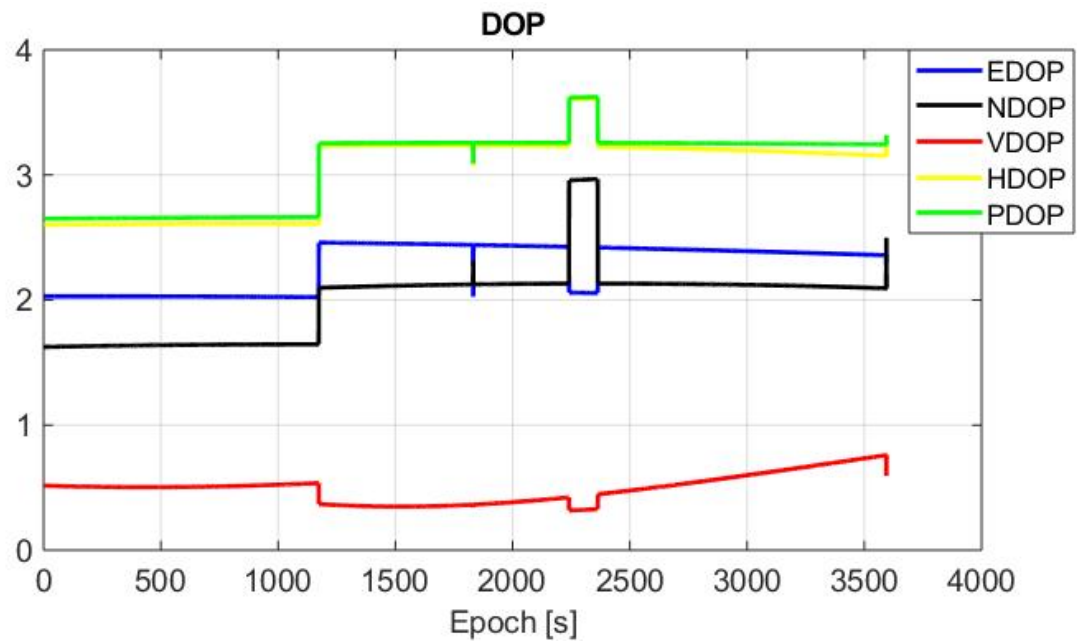


FIGURE 27

Double-differencing DOP plot with highest DOP values

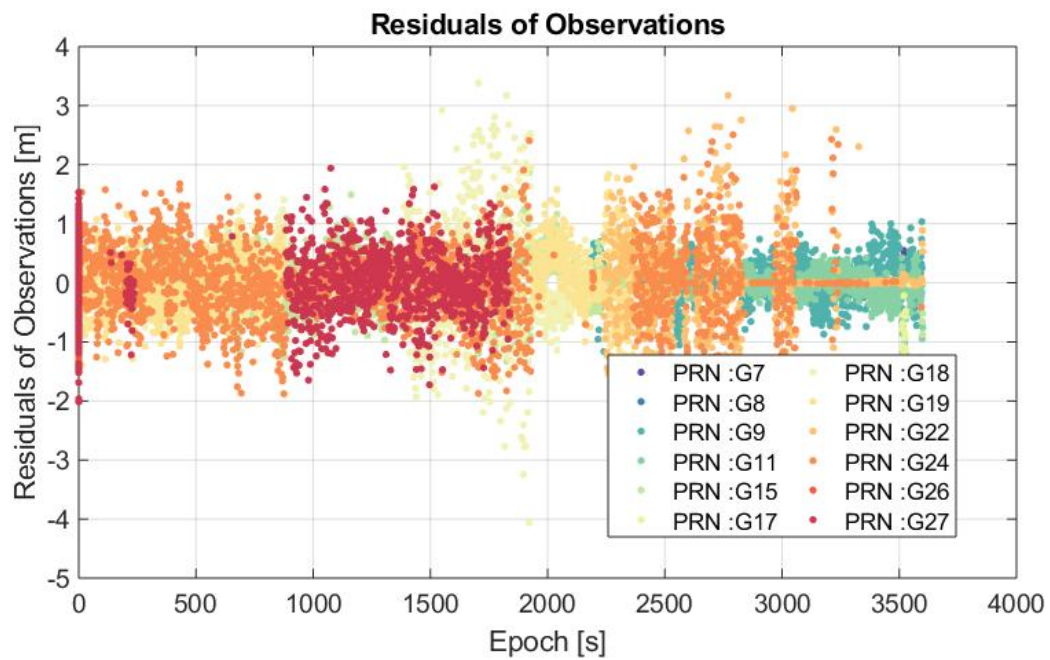
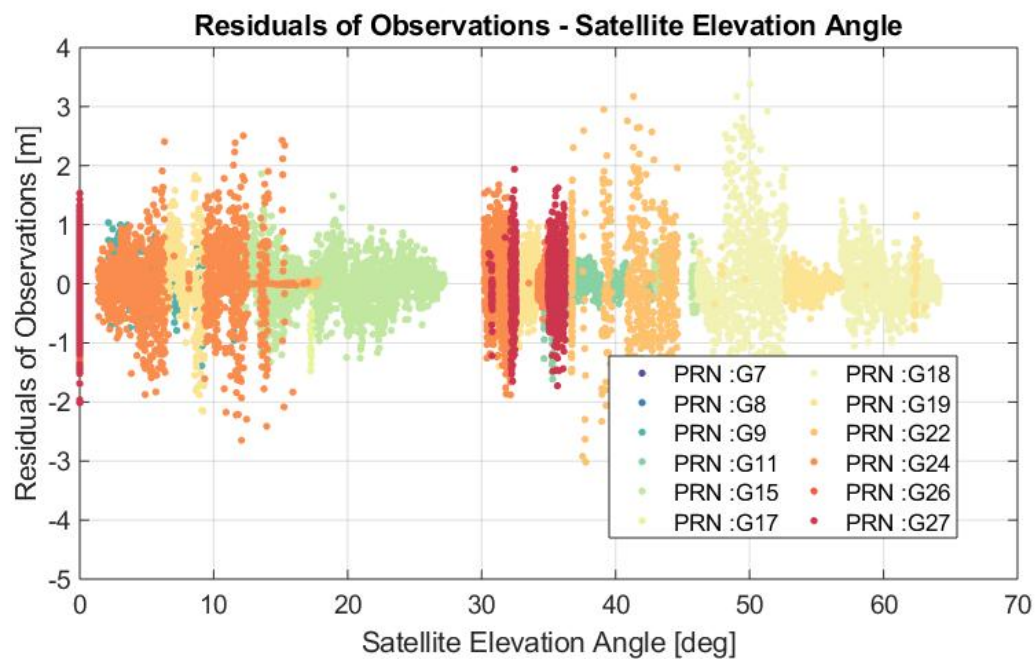


FIGURE 28

Double-differencing residual plot with highest DOP values

**FIGURE 29**

Double-differencing Residual-Elevation plot with highest DOP values

7 Task 7

First, the skyplot (trajectory) of satellites are plotted as a function of azimuth and elevation angle. The result is shown in Figure 30.

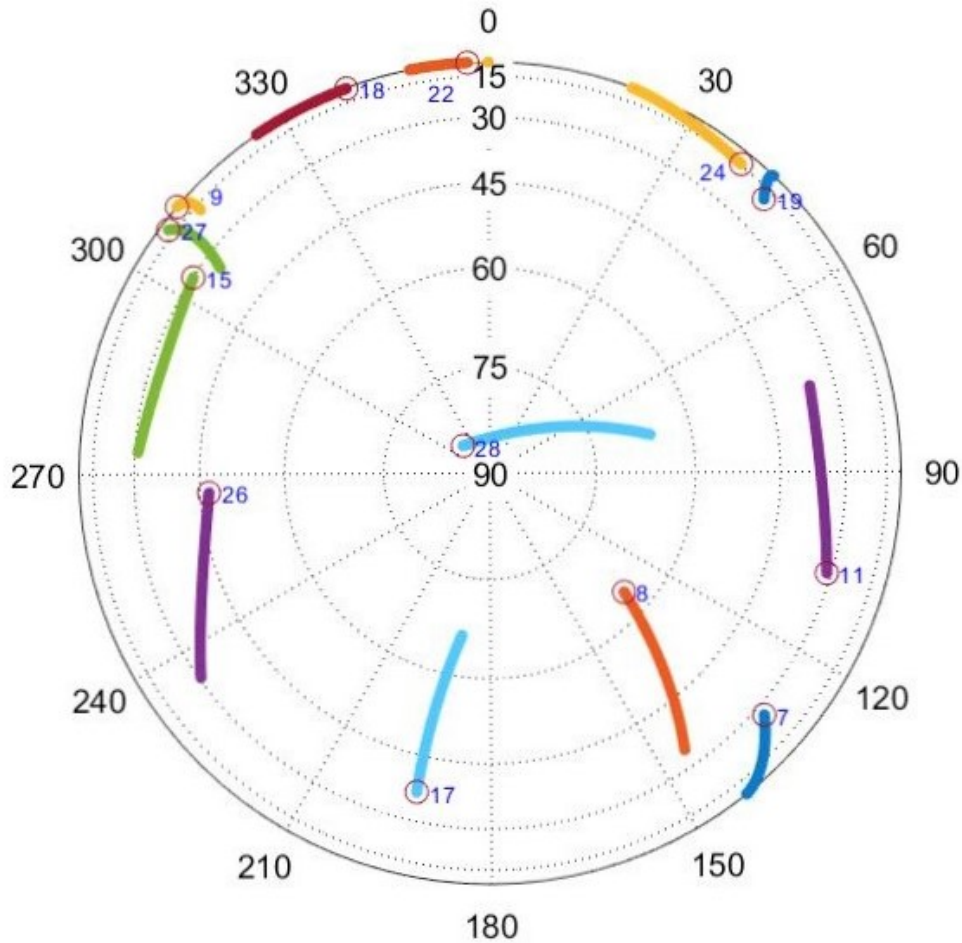


FIGURE 30

Skyplot

Generally speaking, residual can be regraded as a measure of the quality of pseudorange. However, from the residual plots above, we can easily find out that the five-satellite solution's residual are always smaller than the original one. Take Satellite PRN18 as an instance, from Figure 30, it's shown that PRN18 is in a relatively low elevation angle, thus more serious multipath effect and ionospheric errors. The PRN18 residuals in double-differencing solution and five-satellite double-differencing solution are showed in Figure 31, 32 respectively.

By comparing Figure 31 and Figure 32, we can see that the residuals in five-satellite DD solution are way smaller than those of DD solution in the early stage of positioning. In Figure 3, it's shown that the number of visible satellites is always larger 9 which means that there

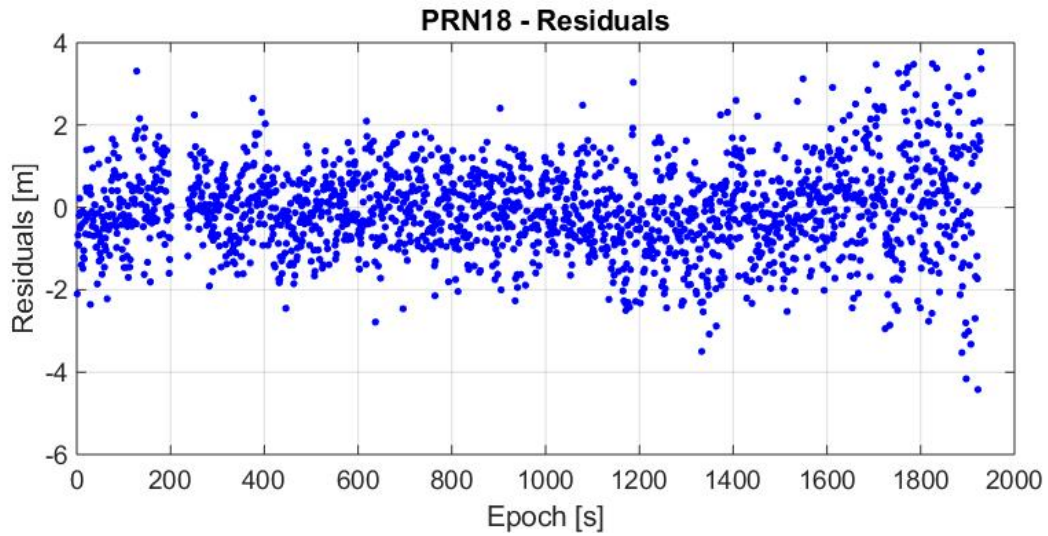


FIGURE 31

PRN18 residuals in double-differencing solution

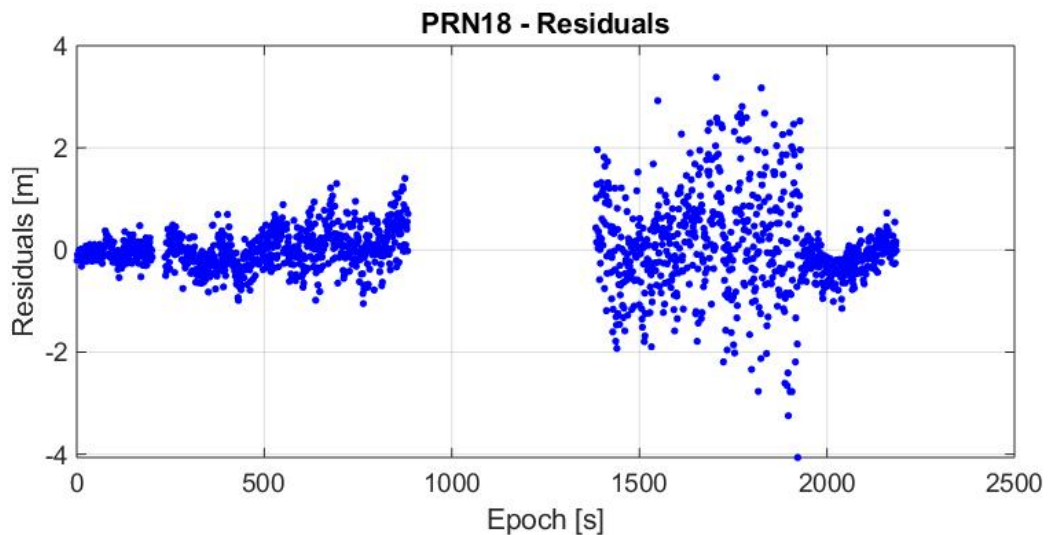


FIGURE 32

PRN18 residuals in five-satellite double-differencing solution

are always enough satellites to provide a solid solution and satellite PRN18 will not be fully trusted in the solution. However, in the five-satellite solution, there are only one redundant observation information in each epoch which means PRN18 plays a more important role in this solution. Thus, the residuals are abnormally small. This situation can be significantly reduced by introducing measurement weight matrix determined by elevation angle and SNR.

From the analysis above, the mean value and standard deviation of true accuracy are concluded in Table 3.

From what has been discussed above, an intuitive conclusion with statistical backup can be drawn:

TABLE 3
Mean value and standard deviation of true accuracy

		East (m)	North (m)	Up (m)
SPP	mean value	1.53	-0.72	-7.44
	standard deviation	0.37	0.85	2.05
5-satellite SPP	mean value	1.74	-1.24	-4.66
	standard deviation	4.03	3.33	14.03
SD	mean value	-0.02	0.10	-0.12
	standard deviation	0.41	0.55	1.07
DD	mean value	-0.01	0.10	-0.14
	standard deviation	0.42	0.73	1.35

1. For GPS constellations, generally speaking, the more visible satellites are, the better the satellite geometry is.
2. The better the satellite geometry is, the more accurate the position solution will be.
3. The better the quality of pseudorange is, the more accurate the position solution will be.